Tetrahedron 69 (2013) 2687–2692

Contents lists available at SciVerse ScienceDirect

Tetrahedron

journal homepage: www.elsevier.com/locate/tet

New emissive organic molecule based on pyrido[3,4-*g*]isoquinoline framework: synthesis and fluorescence tuning as well as optical waveguide behavior

Jianguo Wang, Guanxin Zhang *, Zitong Liu, Xingui Gu, Yongli Yan, Chuang Zhang, Zhenzhen Xu, Yongsheng Zhao, Hongbing Fu, Deqing Zhang *

Beijing National Laboratory for Molecular Sciences, Organic Solids Laboratory and Photochemistry Laboratory, Institute of Chemistry, Chinese Academy of Sciences, Beijing 100190, China

ARTICLE INFO

Article history:
Received 16 November 2012
Received in revised form 3 January 2013
Accepted 4 February 2013
Available online 15 February 2013

Keywords:
Isoquinoline
Solid-state emission
Fluorescence tuning
Optical waveguide

ABSTRACT

In this paper we report the synthesis and crystal structures of emissive organic molecule (**1a**) based on pyrido[3,4-*g*]isoquinoline framework as well as its isomers **1b** and **1c**. The emission quantum yields decrease after transformation of pyridine moieties in **1a** into the cyclic-amides in **1b** and **1c**. The fluorescent spectral results reveal that **1a**, **1b**, and **1c** exhibit no AIE behavior. This is tentatively attributed to intramolecular weak C···H interactions, which may impede the intramolecular rotations based on the crystal structures of **1a** and **1c**. Interestingly, **1a**, **1b**, and **1c** are emissive in the solid state, and among them **1a** possesses the highest emission quantum yield (0.22). Moreover, the fluorescence of **1a** in solution and solid state can be reversibly tuned by reactions with trifluoroacetic acid and triethylamine. Microarea PL studies reveal that microrods of **1a** and these after exposure to HCl gas show typical waveguide behavior.

1. Introduction

Emissive organic molecules have been extensively studied for sensing and molecular imaging for decades. Meanwhile, organic molecules that exhibit strong emission in the solid states have received increasing attention in recent years because of their potential applications in optoelectronic devices such as optical waveguides,[1,2] optically pumped lasers,[3] and light-emitting diodes.[4] However, many luminophores are highly luminescent in solutions, but they become weakly emissive in the solid states. This is usually ascribed to the formation of detrimental species such as excimers and exciplexes in the solid states.[5] In recent years, Tang and his co-workers have reported that siloles,[6] tetraphenylethylenes,[7] and relevant molecules show abnormal fluorescent behaviors; they are weakly or non-emissive in solution, but they become strongly emissive upon formation of aggregation states and in the solid states.[8] This abnormal fluorescent feature was referred to as AIE (aggregation-induced emission). The structural features of siloles and tetraphenylethylenes include at least: (1) the molecules are not planar; (2) the pi-components are connected with sigma-bonds. The internal rotations around these sigma-bonds play a significant role in determining the AIE feature of these molecules. Along this vein many efforts have been taken to explore new molecular frameworks exhibiting AIE behavior.[7–11]

In this paper, we report the synthesis and crystal structures of **1a** with pyrido[3,4-*g*]isoquinoline framework. The initial motivation of this research is to invent new AIE molecules. Compound **1a** entails pi-components connected by sigma-bonds, thus they are potentially AIE molecules according to previous reports.[8a,12] Unfortunately, fluorescent spectral studies reveal that they do not show AIE feature. However, **1a** shows relatively strong emission, which can be tuned by exposure to HCl. Moreover, microrods of **1a** display optical waveguide behavior.

2. Results and discussion

2.1. Synthesis and characterization

The synthesis of **1a**, **1b**, and **1c** started from compound **2**, which was transformed into **3**[13] after reaction with NH_2OH. Compound **3** was allowed to react with $(AcO)_2O$ to yield **4**[14] quantitatively. The Rh-catalyzed oxidative coupling reaction between compound **4** and 1,2-diphenylethyne led to compound **5**. Reaction of **5** with 1-bromohexane in the presence of NaH yielded the O-alkylation product **1a** in 41% yield after separation with column chromatography. Besides **1a** the N-alkylation products **1b** and **1c** were also

* Corresponding authors. Tel.: +86 10 6263 9355; fax: +86 10 6256 2693; e-mail address: dqzhang@iccac.ac.cn (D. Zhang).

0040-4020/$ – see front matter © 2013 Published by Elsevier Ltd.
http://dx.doi.org/10.1016/j.tet.2013.02.041

obtained in 30 and 27% yields, respectively (see Scheme 1). The chemical structures of **1a**, **1b**, and **1c** were confirmed by NMR, MS, IR, and element analysis data (see Experimental section). Moreover, crystal structures of **1a** and **1c** were determined (see below).

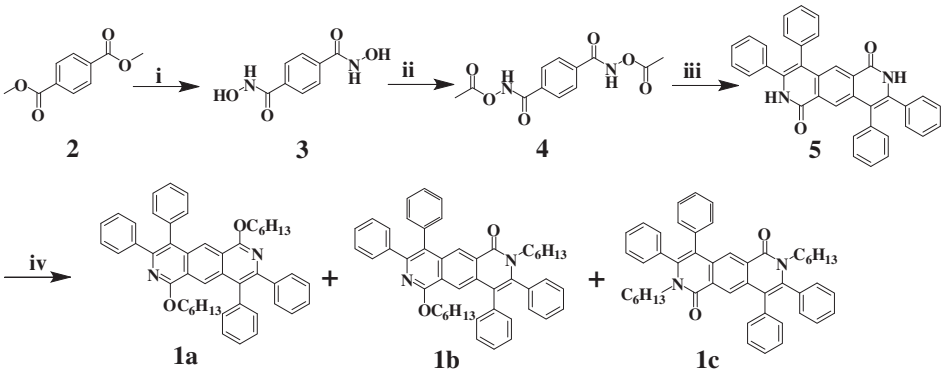

Scheme 1. The chemical structure and synthetic approach for compounds **1a**, **1b**, and **1c**: (i) hydroxylamine hydrochloride, NaOH, H_2O/CH_3OH, rt, 2 h, 95%; (ii) $(AcO)_2O$, CH_2Cl_2, quantitatively; (iii) 1,2-diphenylethyne, $[RhCp^*Cl_2]_2$, CsOAc, CH_3OH, 60 °C, 16 h; (iv) NaH, DMF, 80 °C, overnight.

2.2. Crystal structures

The crystallographic data of **1a** and **1c** were provided in Table S1. Fig. 1 shows the molecular structures of **1a** and **1c**. The bond lengths and angles of **1a** and **1c** are in normal region. The molecular structure of **1a** is central symmetric. The pi-components of **1a** are not coplanar, but the central framework pyrido[3,4-*g*]isoquinoline is almost planar; the phenyl rings C13–C14–C15–C16–C17–C18 and C6–C7–C8–C9–C10–C11 form dihedral angles of 46.68° and 66.26° with the central framework. The distances of C11···H14 and C14···H11 are 3.063 Å and 3.425 Å, respectively; these weak intramolecular interactions may impede the rotations around C5–C6 and C12–C13 bonds. Fig. S1 depicts the intermolecular packing and interactions for **1a**. There are no intermolecular pi–pi interactions, but multiple intermolecular short C···H contacts are available.

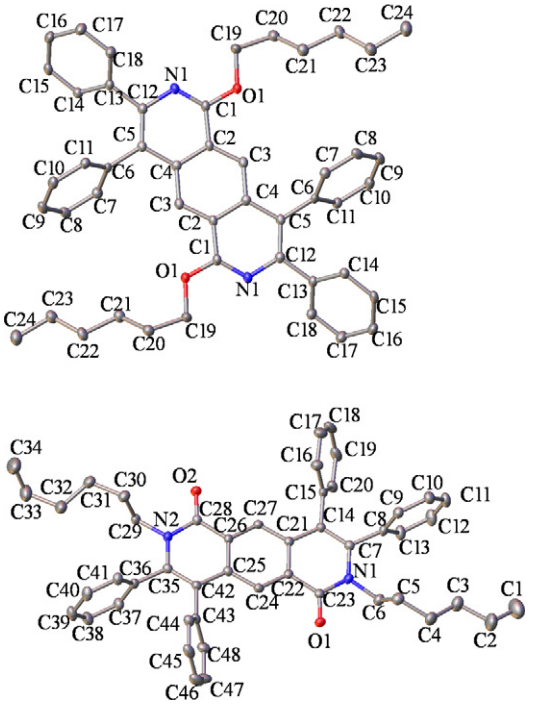

Fig. 1. Molecular structures of **1a** (*up*) and **1c** (*below*); the hydrogen atoms have been omitted for clarity.

The molecular structure of **1c** is not only non-planar, but also non-central symmetric. The four phenyl rings are out of the central framework, which is not fully planar. Intramolecular short interatomic contacts C13–H20 (3.015 Å), C20–H13 (3.292 Å), C7–H20 (3.091 Å), C44–H41 (3.287 Å), C41–H44 (3.045 Å), and C35–H44 (3.131 Å) exist within **1c**; thus, it is also expected that these weak intramolecular interactions are not favorable for the rotations around C7–C8, C14–C15, C35–C36, and C42–C43 bonds. As shown in Fig. S1, multiple intermolecular short C···H contacts exist within crystal of **1c**, but there are no intermolecular pi–pi interactions.

2.3. Emissive properties in solutions and solid states

Compounds **1a**, **1b**, and **1c** show absorptions around 355, 405, and 425 nm as shown in Fig. S2. Table 1 lists the absorption maxima of **1a**, **1b**, and **1c**. Compared to those of **1b** and **1c**, the absorption spectrum of **1a** is slightly red-shifted. In comparison, they all show emissions around 447 and 470 nm (see Fig. 2A). The emission quantum yields of **1a**, **1b**, and **1c** in solution were measured. As listed in Table 1, **1a** is the most strongly emissive with the emission quantum yield of 0.25. It is interesting to note that the emission quantum yields decrease by gradual transformation of pyridine ring in **1a** into the cyclic-amides in **1b** and **1c**. The fluorescence lifetimes of **1a**, **1b**, and **1c** in solution were also measured (see Table 1). They

Table 1
The photophysical properties of **1a**, **1b**, and **1c**

Compounds	Absorption λ_{max} (nm)	Fluorescence λ_{max} (nm) (λ_{ex}=360 nm)	Φ_l[b]	Φ_s[c]	$\langle\tau_l\rangle$[a] (ns)	$\langle\tau_s\rangle$[a] (ns)
1a	278, 362	447, 470	0.25	0.22	5.16	7.867
1b	266, 356	472, 472	0.098	0.07	2.35	2.139
1c	258, 354	469, 469	0.092	0.033	1.43	0.948

[a] An apparent decay time constant $\langle\tau\rangle$ was determined by using the relation $\langle\tau\rangle = \sum_{i=1}^{n} a_i \times \tau_i / \sum_{i=1}^{n} a_i$ (n=1–3), where τ_i and a_i, respectively, represent the individual exponential decay time constant and the corresponding preexponential factor, τ_l is solution state fluorescence lifetime, τ_s is solid-state fluorescence lifetime.

[b] Φ_l represents the respective solution fluorescence quantum efficiency, which was measured using quinine in 1 N H_2SO_4 aqueous solution as the reference (Φ=0.55, λ_{ex}=346 nm).

[c] Φ_s represents the respective solid-state fluorescence quantum efficiency, which was measured with calibrated integrating sphere.

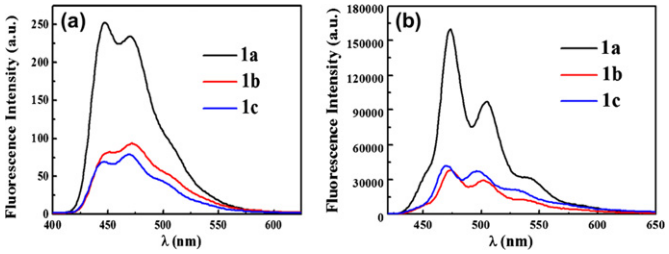

Fig. 2. (A) Fluorescence spectra of compounds **1a**, **1b**, and **1c** (1.0×10^{-5} M) in CH_2Cl_2 (excited at 360 nm); (B) fluorescence spectra of compounds **1a**, **1b**, and **1c** in the solid state (excited at 360 nm).

are all in nanosecond region. As expected, **1a** shows the longest fluorescence lifetime (5.16 ns).

The fluorescence spectra of **1a**, **1b**, and **1c** in THF were also measured after addition of different amounts of water. Unfortunately, no obvious fluorescence enhancement was observed for **1a**, **1b**, and **1c**. Thus, **1a**, **1b**, and **1c** do not exhibit AIE behavior. This is probably due to the intramolecular weak interactions (see above), which may impede the rotations around the sigma-bonds (C5–C6 and C12–C13 in **1a**, C7–C8, C14–C15, C35–C36, and C42–C43 in **1c**) even in solution.

The fluorescence spectra of **1a**, **1b**, and **1c** in the solid state were also measured (see Fig. 2B). Compared to those in solution, the fluorescence spectra of **1a**, **1b**, and **1c** in the solid state are slightly red-shifted. For instance, the emission maximum of **1a** is shifted from 447 to 470 nm in solution to 473 and 505 nm, respectively, in the solid state. The emission quantum yields and fluorescence lifetimes of **1a**, **1b**, and **1c** in the solid state were also measured and listed in Table 1. Compounds **1a**, **1b**, and **1c** are comparably emissive in the solid state as the respective solutions of **1a**, **1b**, and **1c**. This agrees well with the observation that their average fluorescence lifetimes in the solid state are also relatively long (see Table 1). The following structural features may attribute to the relatively strong fluorescence of **1a**, **1b**, and **1c** in the solid state: (1) molecules of **1a**, **1b**, and **1c** are non-planar, thus intermolecular pi–pi interactions are not favorable (see Fig. S1); (2) intermolecular multiple C···H interactions will reduce the non-radiative pathways to enhance the emission efficiency.

2.4. Tuning the fluorescence of 1a by addition of acid and base

Interestingly, the fluorescence of **1a** can be tuned by addition of acid. As depicted in Fig. 3, the fluorescence of **1a** becomes gradually weak and red-shifted after addition of different amounts of trifluoroacetic acid (TFA). For instance, the emission intensity at 470 nm is reduced by ca. 1500 folds, and the emission maximum is shifted from 470 to 555 nm after addition of 20 equiv of TFA. Such fluorescence change can be detected with naked-eye as illustrated in inset of Fig. 3, where the photos of the solutions of **1a** under UV light irradiation were displayed in the absence and presence of TFA. Simultaneously, the absorption spectrum of **1a** is changed upon addition of TFA; the absorptions at 356, 405, and 426 nm are gradually reduced and a new absorption tail till 500 nm emerges (see Fig. S3). The fluorescence responsiveness of **1a** toward TFA is likely due to the protonation of pyridine moieties in **1a**. Moreover, the fluorescence of **1a** can be restored by further addition of triethylamine as shown in Fig. 4. Therefore, the fluorescence of **1a** in solution can be reversibly tuned by addition of acid and base.

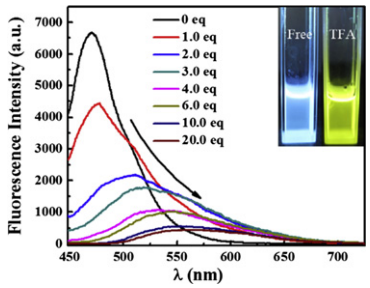

Fig. 3. Fluorescence spectra of **1a** (1.0×10^{-3} M) in CH_2Cl_2 after addition of different amounts of TFA (0–20.0 equiv) with $\lambda_{ex.}$=438 nm; inset shows the photos of CH_2Cl_2 solution of **1a** (1.0×10^{-3} M) in the absence or presence of TFA under UV light (365 nm) irradiation.

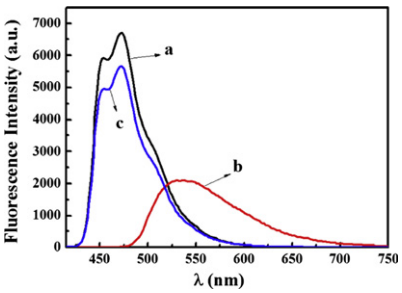

Fig. 4. Fluorescence spectra of CH_2Cl_2 solution of **1a** (1.0×10^{-3} M): (a) **1a** only, (b) **1a**+TFA (20.0 equiv), (c) **1a**+TFA (20.0 equiv)+triethylamine (20.0 equiv); the excitation wavelength was 360 nm.

The fluorescence of **1a** in the solid state also shows responsiveness toward acid. Fig. 5A depicts the variation of the fluorescence spectrum of **1a** upon exposure to HCl gas of different concentrations. Similarly, the solid fluorescence intensity becomes weak and red-shifted by increasing the concentration of HCl gas. The emission color of **1a** in the solid state is changed from blue to green after exposure to HCl gas (320,000 ppm) as illustrated in Fig. 5B and C, where PL (photo-luminescence) images after exposure **1a** to HCl gas (320,000 ppm) for 5 min are displayed. However, the fluorescence of **1a** in the solid state can be restored by just letting the solid of **1a** that was treated with HCl gas in air for 30 min.

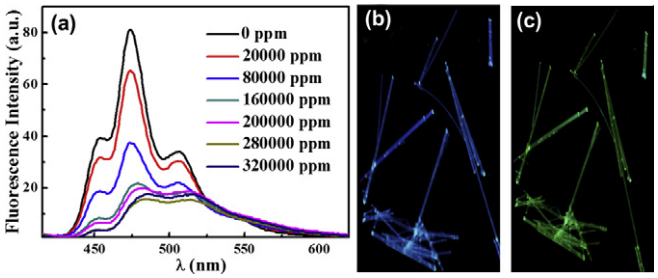

Fig. 5. (A): Solid-state fluorescence spectra of **1a** upon exposure to different concentrations of HCl gas for 5.0 min. (B) and (C): PL images of **1a** before (B) and after (C) exposure to HCl gas (320,000 ppm) for 5.0 min.

2.5. Waveguide behavior of microrods of 1a

The microrods of **1a**, which were prepared by evaporation of the solution of **1a** in CH_2Cl_2/MeOH (v/v, 5:1), were excited with a focused laser down to the diffraction limit at different local positions along the length of the microrods. Fig. 6A depicts the microarea PL (photoluminescence) microscopic images for microrods of **1a**. Interestingly, blue-green emission was detected from both ends of the microrods of **1a** irrespective of the excitation position. In

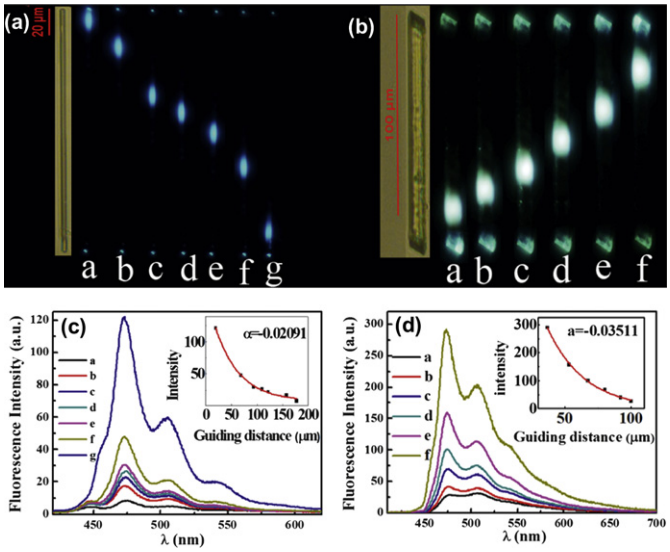

Fig. 6. Bright-field and microarea PL images of compound **1a**, by exciting the microrod from different positions, (A) before and (B) after exposure to HCl gas; spatially resolved PL spectra of outcoupled light at a distance of a, b, c, d, e, f, and g (curves from bottom to top) from the tip of a single microrod, recorded by focused 351 nm laser excitation, (C) before exposure to HCl gas, (D) after exposure to HCl gas; the insets show the variation plot of the fluorescence intensities at 472 and 473 nm versus the propagation distance.

general, the emission of light can only be observed at the local area of the excited position. The appearance of the outcoupling light at the ends of each microrod of **1a** is a typical characteristic of waveguide behavior.

The spatially resolved PL spectra were measured in order to gain further insight into the light waveguide behavior within microrods of **1a**. Fig. 6C shows the collected PL spectra at the end of a single microrod of **1a** under the excitations at different positions (labeled as a, b, c, d, e, f, and g). The emission spectra upon excitation at different positions kept almost unaltered. But, the emission intensity at the microrod-ends decreased upon increasing the propagation distance. As depicted in the inset of Fig. 6C, the emission intensity at 472 nm of the outcoupled light decreased almost exponentially with the propagation distance. Note that the emission intensities of the excited points do not change substantially with the position along the microrods. Thus, the inset of Fig. 6C can also represent the variation of intensity ratio of incident and outcoupled light versus the propagation distance. By fitting the data of inset of Fig. 6C according to the reported procedure,[15] the optical loss coefficient at 472 nm for microrods of **1a** was estimated to be 20.91 dB/mm. Based on the fact that the collected PL spectra at the end of a single microrod of **1a** under the excitations at different positions are almost the same, self-absorption may not contribute largely to the optical loss during the light propagation. Thus, it is assumed that the substrate effect and Rayleigh scattering may induce the optical loss observed for microrod of **1a**, according to previous studies.[1,2,16]

As discussed above, the blue-green emission of **1a** in the solid state is changed to green emission upon exposure to HCl gas. Interestingly, microrods of **1a** after treatment with HCl gas also show typical optical waveguide behavior. As shown in Fig. 6B, where the microarea PL microscopic images of the microrod of **1a** after exposure to HCl gas (320,000 ppm) were displayed, green luminescence spots at both tips and relatively weaker emission from the bodies of the microrod were detected. Fig. 6D shows the collected PL spectra at the end of a single microrod of **1a** after exposure to HCl gas under the excitations at different positions (labeled as a, b, c, d, e, and f). Again, the fluorescence intensity decreased by prolonging the propagation distance as depicted in the inset of Fig. 6D. Similarly, the optical loss coefficient at 473 nm was estimated to be 35.11 dB/mm.

3. Conclusion

A new emissive organic molecule (**1a**) based on pyrido[3,4-*g*] isoquinoline framework as well as its isomers **1b** and **1c** are reported. The emission quantum yields decrease after transformation of pyridine moieties in **1a** into the cyclic-amides in **1b** and **1c**. Compounds **1a**, **1b**, and **1c** exhibit no AIE behavior. This may be due to intramolecular weak C···H interactions, which may impede the intramolecular rotations based on the crystal structures of **1a** and **1c**. Interestingly, **1a**, **1b**, and **1c** are emissive in the solid state, and among them **1a** possesses the highest emission quantum yield (0.22). Moreover, the fluorescence of **1a** in solution and solid state can be reversibly tuned by reactions with acid and base. Microarea PL studies reveal that microrods of **1a** show typical waveguide behavior with blue-green emission at the ends of microrods, and these microrods after exposure to HCl gas also exhibit optical waveguide property with green emission at the ends of microrods.

4. Experimental section

4.1. General method

All chemical materials were purchased from Alfa Aesar, Sigma–Aldrich or TCI for direct use. The water used was purified by Millipore filtration system. Melting points were measured with Büchi B540. ^{1}H NMR and ^{13}C NMR were collected on Bruker Avance 400-MHz spectrometer. MALDI-TOF mass spectra were recorded with BEFLEX III spectrometer. Absorption spectra were recorded on UV–vis–NIR spectrophotometer (UV-3600, Shimadzu spectrometer). Steady-state fluorescence spectra were recorded with Hitachi (F-4500) spectrophotometers at 25 °C. The IR spectra were measured on the IR spectrometer (TENSOR-27). PL images were recorded with Olympus research inverted system microscope (FV1000-IX81, Tokyo, Japan) equipped with a charge couple device (CCD, Olympus DP71, Tokyo, Japan) camera; the excitation source is a Hg lamp equipped with a band-pass filter (330–380 nm). All photographs were recorded on a Canon digital camera.

4.2. Crystal structural analysis

Crystals of **1a** and **1c** were grown by slow evaporation from the dichloromethane/methanol mixed solution. All single crystals data were collected on Rigaku Saturn diffractometer with CCD area detector. All calculations were performed using the SHELXL97 and crystal structure crystallographic software packages. Crystallographic data (excluding structure factors) for the structure(s) reported in this paper have been deposited with the Cambridge Crystallographic Data Centre as supplementary publication no. CCDC: 905697 for **1a** and 905698 for **1c**.

4.3. Photophysical studies

Fluorescence quantum efficiencies of **1a**, **1b**, and **1c** in the solids states were recorded on FLSP 920 fluorescence spectroscopy with a calibrated integrating sphere system. Fluorescence lifetimes of **1a**, **1b**, and **1c** (both the solution state and the solid state) were measured based on the time-resolved PL experiments, which were made with a regenerative amplified Ti:sapphire laser (Spectra-Physics, Spitfire) at 400 nm. The PL spectra were recorded with a streak camera (C5680, Hamamatsu Photonics) attached to a polychromator (Chromex, Hamamatsu Photonics), for which the

temporal and spectral resolutions of the detector are ~10 ps and 2 nm, respectively. All the spectroscopic measurements were carried out at room temperature.

4.4. Optical waveguide measurements

To measure the microarea PL spectra of single microrod, the microrods dispersed on a glass cover-slip were excited with an UV laser (λ=351 nm, Beamlok, Spectra-physics). The excitation laser was filtered with a band-pass filter (330–380 nm), then focused to excite the microrod with an objective (50×, N.A.=0.80). After passing through a narrow band filter (LD01-405, Semrock), the excitation laser was focused on the sample by the same objective and the spot size was less than 2 μm. The collected microarea PL emission was filtered by a long-pass filter (BA420), and coupled to a grating spectrometer (Acton, SP-2358) with matched ProEm: 512B EMCCD camera (Princeton Instruments).

4.5. Synthesis and characterization

*4.5.1. Synthesis of compound **5**.* Compound **4** (1.0 g, 3.57 mmol), 1,2-diphenylethyne (1.39 g, 7.85 mmol), $[Cp^*RhCl_2]_2$ (110 mg, 5 mol %), and CsOAc (2.05 g, 10.7 mmol) were added to a round bottom flask. Then, MeOH (30 mL) was added. The reaction mixture was stirred at 60 °C for 16 h. Afterward, the mixture was filtered, and the solid was washed with water and CH_2Cl_2.The residue was dried under reduced pressure to afford compound **5** as a light-yellow solid, which was used for the next step without further purification for its poor solubility; MS (MALDI-TOF): 517 ($M+H^+$), 539 ($M+Na^+$).

*4.5.2. Synthesis of compounds **1a**, **1b**, and **1c**.* To a DMF solution (5 mL) of compound **5** (120 mg, 0.23 mmol), NaH (60%) (23 mg, 0.58 mmol)[17] was added, and the mixture was stirred at 0 °C for 1.0 h. Then, 1-bromohexane (95 mg, 0.58 mmol) was added via a syringe. The mixture was heated to 80 °C for 3.0 h. Dichloromethane (30 mL) and H_2O (20 mL) were added. The organic layer was washed with brine (15 mL×3), and dried with Na_2SO_4. After evaporation of the solvent under vacuum, the residue was subjected to flash column chromatography with dichloromethane/petroleum ether (60–90 °C) (v/v, 4:1 to 1:1) as eluent to afford the desired product (**1a**, **1b**, and **1c**).

*4.5.2.1. Compound **1a**.* Yield: 41%; mp 231.2–232 °C; ν_{FTIR} (KBr) 3054, 2956, 2926, 2855, 1591, 1573, 1537, 1423, 1339, 1300, 1211, 1147, 1072, 909, 701 cm^{-1}; ^1H NMR (400 MHz, $CDCl_3$): δ (ppm) 8.60 (2H, s), 7.47–7.38 (10H, m), 7.34–7.32 (4H, m), 7.21–7.18 (6H, m), 4.57 (4H, t, J=6.4 Hz), 1.82–1.78 (4H, m), 1.46–1.43 (4H, m), 1.35–1.33 (8H, m), 0.92 (6H, t, J=6.8 Hz). ^{13}C NMR (100 MHz, $CDCl_3$): δ (ppm) 159.60, 145.40, 140.55, 137.78, 135.44, 131.75, 130.44, 128.42, 127.46, 127.18, 127.06, 124.49, 121.77, 120.51, 66.45, 31.63, 28.85, 25.95, 22.69, 14.13. MALDI-TOF: 685.5 $[M+H]^+$. Anal. Calcd for $C_{48}H_{48}N_2O_2$: C, 84.17; H, 7.06; N, 4.09. Found: C, 83.71; H, 6.84; N, 4.09.

*4.5.2.2. Compound **1b**.* Yield 30%; mp 204.9–205.6 °C; ν_{FTIR} (KBr) 3054, 2954, 2925, 2856, 1648, 1612, 1593, 1558, 1428, 1341, 1320, 1299, 1229, 1030, 701 cm^{-1}; ^1H NMR (400 MHz, $CDCl_3$) δ (ppm) 8.86 (s, 1H), 8.11 (s, 1H), 7.45–7.34 (m, 5H), 7.29 (d, J=7.8 Hz, 2H), 7.25–7.12 (m, 13H), 4.52 (t, J=6.2 Hz, 2H), 3.80 (t, J=6.2 Hz, 2H), 1.81–1.71 (m, 2H), 1.59 (s, 2H), 1.37 (s, 2H), 1.33–1.23 (m, 4H), 1.19–1.10 (m, 2H), 1.07 (d, J=2.8 Hz, 4H), 0.89 (t, J=6.4 Hz, 3H), 0.77 (t, J=7.1 Hz, 3H). ^{13}C NMR (100 MHz, $CDCl_3$) δ (ppm) 162.30, 159.34, 146.19, 140.59 9, 140.45, 137.46, 136.49, 135.98, 134.76, 134.17, 131.67, 131.57, 130.39, 128.63, 128.24, 127.94, 127.90, 127.43, 127.32, 127.04, 126.87, 126.37, 125.02, 121.35, 120.97, 119.21, 66.32, 46.45, 31.56, 31.04, 28.80, 28.56, 26.49, 25.86, 22.64, 22.37, 14.10, 13.91. MALDI-TOF: 684.4 $[M]^+$. Anal. Calcd for $C_{48}H_{48}N_2O_2$: C, 84.17; H, 7.06; N, 4.09. Found: C, 83.95; H, 7.03; N, 4.13.

*4.5.2.3. Compound **1c**.* Yield 27%; mp 309.0–310.2 °C; ν_{FTIR} (KBr) 3059, 2954, 2929, 2856, 1641, 1588, 1492, 1442, 1370, 1345, 1326, 1299, 1074, 698 cm^{-1}; ^1H NMR (400 MHz, $CDCl_3$): δ (ppm) 8.40 (s, 2H), 7.23–7.15 (m, 16H), 7.10 (d, J=6.7 Hz, 4H), 3.77 (d, J=7.8 Hz, 4H), 1.56 (s, 4H), 1.19–0.99 (m, 12H), 0.76 (t, J=7.1 Hz, 6H). ^{13}C NMR (100 MHz, $CDCl_3$): δ (ppm) 161.98, 140.87, 136.14, 134.75, 134.67, 131.48, 130.34, 128.21, 128.13, 127.86, 127.01, 125.84, 119.45, 46.53, 31.00, 28.50, 26.47, 22.35, 13.89. MALDI-TOF: 684.5 $[M]^+$. Anal. Calcd for $C_{48}H_{48}N_2O_2$: C, 84.17; H, 7.06; N, 4.09. Found: C, 84.13; H, 6.76; N, 4.13.

Acknowledgements

The present research was financially supported by Chinese Academy of Sciences, NSFC, and State Key Basic Research Program.

Supplementary data

Absorption spectra, fluorescence lifetime fitting curves, crystals data and ^1H and ^{13}C NMR spectra, for **1a**, **1b** or **1c**. Supplementary data associated with this article can be found in the online version, at http://dx.doi.org/10.1016/j.tet.2013.02.041.

References and notes

1. (a) Tong, L. M.; Gattass, R. R.; Ashcom, J. B.; He, S. L.; Lou, J. Y.; Shen, M. Y.; Maxwell, I.; Mazur, E. *Nature* **2003**, *426*, 816; (b) Takazawa, K.; Kitahama, Y.; Kimura, Y.; Kido, G. *Nano Lett.* **2005**, *5*, 1293; (c) Wang, X.; Zhou, Y.; Lei, T.; Hu, N.; Chen, E. Q.; Pei, J. *Chem. Mater.* **2010**, *22*, 3735.
2. (a) Zhang, C.; Zhao, Y. S.; Yao, J. N. *Phys. Chem. Chem. Phys.* **2011**, *13*, 9060; (b) Liao, Q.; Fu, H. B.; Yao, J. N. *Adv. Mater.* **2009**, *21*, 4153; (c) Zheng, J. Y.; Yan, Y. L.; Wang, X. P.; Zhao, Y. S.; Huang, J. X.; Yao, J. N. *J. Am. Chem. Soc.* **2012**, *134*, 2880; (d) Lei, Y. L.; Liao, Q.; Fu, H. B.; Yao, J. N. *J. Am. Chem. Soc.* **2010**, *132*, 1742.
3. (a) Bulović, V.; Kozlov, V. G.; Khalfin, V. B.; Forrest, S. R. *Science* **1998**, *279*, 553; (b) Duan, X. F.; Huang, Y.; Agarwal, R.; Lieber, C. M. *Nature* **2003**, *421*, 241; (c) Zhao, Y. S.; Peng, A. D.; Fu, H. B.; Ma, Y.; Yao, J. N. *Adv. Mater.* **2008**, *20*, 1661; (d) Samuel, I. D. W.; Turnbull, G. A. *Chem. Rev.* **2007**, *107*, 1272.
4. (a) Figueira-Duarte, T. M.; Müllen, K. *Chem. Rev.* **2011**, *111*, 7260; (b) Aziz, H.; Popovic, Z. D.; Hu, N. X.; Hor, A. M.; Xu, G. *Science* **1999**, *283*, 1900; (c) Yuan, W. Z.; Lu, P.; Chen, S. M.; Lam, J. W. Y.; Wang, Z. M.; Liu, Y.; Kwok, H. S.; Ma, Y. G.; Tang, B. Z. *Adv. Mater.* **2010**, *22*, 2159; (d) Lee, J. H.; Yuan, Y. Y.; Kang, Y. J.; Jia, W. L.; Lu, Z. H.; Wang, S. N. *Adv. Funct. Mater.* **2006**, *16*, 681; (e) Tang, M. L.; Bao, Z. N. *Chem. Mater.* **2011**, *23*, 446; (f) Darwish, T. A.; Smith, A. R. G.; Gentle, I. R.; Burn, P. L.; Luks, E.; Moraes, G.; Gillon, M.; Holden, P. J.; James, M. *Tetrahedron Lett.* **2012**, *53*, 931; (g) Park, H.; Rao, Y. L.; Varlan, M.; Kim, J.; Ko, S. B.; Wang, S. N.; Kang, Y. J. *Tetrahedron* **2012**, *68*, 9278; (h) Omar, W. A. E.; Haverinen, H.; Hormi, O. E. O. *Tetrahedron* **2009**, *65*, 9707.
5. (a) Friend, R. H.; Gymer, R. W.; Holms, A. B.; Burroughes, J. H.; Marks, R. N.; Taliani, C. D.; Bradley, D. C.; Dos Santos, D. A.; Brédas, J. L.; Lögdlund, M.; Salaneck, W. R. *Nature* **1999**, *397*, 121; (b) Jenekhe, S. A.; Osaheni, J. A. *Science* **1994**, *265*, 765; (c) Yin, S. W.; Peng, Q.; Shuai, Z. *Phys. Rev. B* **2006**, *73*, 205409; (d) Birks, J. B. *Photophysics of Aromatic Molecules*; Wiley: London, UK, 1970.
6. (a) Qi, X. Y.; Li, H.; Lam, J. W. Y.; Yuan, X. T.; Wei, J.; Tang, B. Z.; Zhang, H. *Adv. Mater.* **2012**, *24*, 4191; (b) Li, Z.; Dong, Y. Q.; Lam, J. W. Y.; Sun, J. X.; Qin, A. J.; Häußler, M.; Dong, Y. P.; Sung, H. H. Y.; Williams, I. D.; Kwok, H. S.; Tang, B. Z. *Adv. Funct. Mater.* **2009**, *19*, 905; (c) Mahtab, F.; Yu, Y.; Lam, J. W. Y.; Liu, J. Z.; Zhang, B.; Lu, P.; Zhang, X. X.; Tang, B. Z. *Adv. Funct. Mater.* **2011**, *21*, 1733; (d) Yu, G.; Yin, S. W.; Liu, Y. Q.; Chen, J. S.; Xu, X. J.; Sun, X. B.; Ma, D. G.; Zhan, X. W.; Peng, Q.; Shuai, Z. G.; Tang, B. Z.; Zhu, D. B.; Fang, W. H.; Luo, Y. *J. Am. Chem. Soc.* **2005**, *127*, 6335; (e) Luo, J. D.; Xie, Z. L.; Lam, J. W. Y.; Cheng, L.; Chen, H. Y.; Qiu, C. F.; Kwok, H. S.; Zhan, X. W.; Liu, Y. Q.; Zhu, D. B.; Tang, B. Z. *Chem. Commun.* **2001**, 1740.
7. (a) Chen, Q.; Zhang, D. Q.; Zhang, G. X.; Yang, X. Y.; Feng, Y.; Fan, Q. H.; Zhu, D. B. *Adv. Funct. Mater.* **2010**, *20*, 3244; (b) Chan, C. Y. K.; Zhao, Z. J.; Lam, J. W. Y.; Liu, J. Z.; Chen, S. M.; Lu, P.; Mahtab, F.; Chen, X. J.; Sung, H. H. Y.; Kwok, H. S.; Ma, Y. G.; Williams, I. D.; Wong, K. S.; Tang, B. Z. *Adv. Funct. Mater.* **2012**, *22*, 378.
8. (a) Hong, Y.; Lam, J. W. Y.; Tang, B. Z. *Chem. Soc. Rev.* **2011**, *40*, 5361; (b) Zhang, Z. Y.; Xu, B.; Su, J. H.; Shen, L. P.; Xie, Y. S.; Tian, H. *Angew. Chem., Int. Ed.* **2011**, *50*, 11654; (c) Wang, B.; Wang, Y. C.; Hua, J. L.; Jiang, Y. H.; Huang, J. H.; Qian, S. X.; Tian, H. *Chem.—Eur. J.* **2011**, *17*, 2647; (d) Jiang, Y. H.; Wang, Y. C.; Hua, J. L.; Tang, J.; Li, B.; Qian, S. X.; Tian, H. *Chem. Commun.* **2010**, 4689; (e) Tam, Y. Y.; Wong, K. M. C.; Yam, V. W. *J. Am. Chem. Soc.* **2009**, *131*, 6253; (f) Oelkrug, D.; Tompert, A.; Gierschner, J.; Egelhaaf, H. J.; Hanack, M.; Hohloch, M.; Steinhuber, E. *J. Phys. Chem. B* **1998**, *102*, 1902.

9. (a) Hu, R. R.; Maldonado, J. L.; Rodriguez, M.; Deng, C. M.; Jim, C. K. W.; Lam, J. W. Y.; Yuen, M. M. F.; Ramos-Ortiz, G.; Tang, B. Z. *J. Mater. Chem.* **2012**, *22*, 232; (b) Zhao, Z. J.; Chen, S. M.; Shen, X. Y.; Mahtab, F.; Yu, Y.; Lu, P.; Lam, J. W. Y.; Kwoka, H. S.; Tang, B. Z. *Chem. Commun.* **2010**, 686; (c) Tseng, N. W.; Liu, J. Z.; Ng, J. C. Y.; Lam, J. W. Y.; Sung, H. H. Y.; Williamsa, I. D.; Tang, B. Z. *Chem. Sci.* **2012**, *3*, 493; (d) Yuan, W. Z.; Chen, S. M.; Lam, J. W. Y.; Deng, C. M.; Lu, P.; Sung, H. H. Y.; Williams, I. D.; Kwok, H. S.; Zhang, Y. M.; Tang, B. Z. *Chem. Commun.* **2011**, 11216.
10. (a) Ning, Z. J.; Chen, Z.; Zhang, Q.; Yan, Y. L.; Qian, S. X.; Cao, Y.; Tian, H. *Adv. Funct. Mater.* **2007**, *17*, 3799; (b) Kapadia, P. P.; Widen, J. C.; Magnus, M. A.; Swenson, D. C.; Pigge, F. C. *Tetrahedron Lett.* **2011**, *52*, 2519; (c) Ooyama, Y.; Nabeshima, S.; Mamura, T.; Ooyama, H. E.; Yoshida, K. *Tetrahedron* **2010**, *66*, 7954.
11. Yang, Y.; Su, X.; Carrollb, C. N.; Aprahamian, I. *Chem. Sci.* **2012**, *3*, 610.
12. (a) Hong, Y.; Lam, J. W. Y.; Tang, B. Z. *Chem. Commun.* **2009**, 4332; (b) Tong, H.; Hong, Y.; Dong, Y.; Ren, Y.; Haeussler, M.; Lam, J. W. Y.; Wong, K. S.; Tang, B. Z. *J. Phys. Chem. B* **2007**, *111*, 2000; (c) Zeng, Q.; Li, Z.; Dong, Y.; Di, C.; Qin, A.; Hong, Y.; Ji, L.; Zhu, Z.; Jim, C. K. W.; Yu, G.; Li, Q.; Li, Z.; Liu, Y.; Qin, J.; Tang, B. Z. *Chem. Commun.* **2007**, 70; (d) Wang, M.; Zhang, G. X.; Zhang, D. Q.; Zhu, D. B.; Tang, B. Z. *J. Mater. Chem.* **2010**, *20*, 1858.
13. Griffith, D.; Krot, K.; Comiskey, J.; Nolan, K. B.; Marmion, C. J. *Dalton Trans.* **2008**, 137.
14. Hynes, J. B. *J. Med. Chem.* **1970**, *13*, 1235.
15. Barrelet, C. J.; Greytak, A. B.; Lieber, C. M. *Nano Lett.* **2004**, *4*, 1981.
16. (a) Bureev, S. V.; Meshkovskii, I. K.; Utkin, E. Yu.; Dukel'skii, K. V.; Eron'yan, M. A.; Komarov, A. V.; Romashova, E. I.; Serkov, M. M.; Bisyarin, M. A. *J. Opt. Technol.* **2012**, *79*, 433; (b) Eaton, S. M.; Chen, W. J.; Zhang, H. B.; Iyer, R.; Li, J. Z.; Ng, M. L.; Ho, S.; Aitchison, J. S.; Herman, P. R. *J. Lightwave Technol.* **2009**, *27*, 1079; (c) Batista, R. M. F.; Costa, S. P. G.; Malheiro, E. L.; Belsley, M.; Raposo, M. M. M. *Tetrahedron* **2007**, *63*, 4258.
17. *n*-BuLi and LDA were also used in the introduction of hexane fragment. However, the results indicated that the yield of **1a** was not enhanced when LDA or *n*-BuLi was applied under the same reaction conditions. Compounds **1a**, **1b**, and **1c** were obtained in 25, 20, and 12% yields, respectively, when *n*-BuLi was used as the base. Similarly, **1a**, **1b**, and **1c** were yielded in 35, 28, and 20% yields, respectively, when LDA was applied.